Design of a Microwave Breast Imaging Array Composed of Dual-Band Miniaturized Antennas

S. M. Aguilar, M. A. Al-Joumayly, J. D. Shea, N. Behdad, and S. C. Hagness

Department of Electrical and Computer Engineering, University of Wisconsin, Madison, WI 53706 USA
E-mail: smaguilar@wisc.edu; aljoumayly@wisc.edu; jshea1@wisc.edu; behdad@wisc.edu; hagness@engr.wisc.edu.

Abstract

We present a compact dual-band patch antenna array designed for use in a 3-D microwave tomography system for breast imaging. The array is designed for operation within the interstitial space of an MRI patient support platform. This configuration permits scattered-field data acquisition with the breast in the same position as a benchmark MRI scan, thereby enabling precise co-registration with breast MRI. We investigate operating characteristics of the antenna array elements contained in the array using numerical simulations. We demonstrate that dual-band operation of the array is maintained in the presence of an ellipsoidal breast phantom.

1. Introduction

Microwave breast imaging is a low-cost, non-ionizing, three-dimensional (3-D) tomographic technology that has the potential for improving breast cancer screening and diagnosis [1]-[4]. The microwave tomography scan involves transmitting low-power microwave signals into the breast using an array of antennas. The array also measures the scattered signals that are used to reconstruct the spatial distribution of the dielectric properties throughout the breast volume.

Validating microwave imaging as a viable tool for breast imaging requires unambiguous co-registration with a clinical benchmark such as magnetic resonance imaging (MRI). In this paper, we present the design of a microwave antenna array that will enable an objective and precise comparison to be made between microwave and MR images of the breast. Our proposed system configuration exploits a novel breast MRI system with coils that can be removed from the patient support platform (shown in Fig. 1) to create space for a microwave antenna array. This approach enables the microwave scan to take place with the patient on the MRI couch, but outside of the MRI bore. A thermoplastic mesh is used to maintain the position of the breast for both MRI and microwave scans [5].

Figure 1: Photograph of the patient support platform positioned on top of a standard MRI couch.

The design of the 3-D antenna array is constrained by the limited vertical extent (~13 cm) available in the patient support platform. The design is also influenced by consideration of factors that impact microwave imaging quality, including the number of frequencies used for data acquisition [6], the number and location of observations of the scattered fields [6], and the efficiency of coupling of low-power signals into the breast. Specifically, the array antenna elements should operate at multiple frequencies to alleviate the inherent challenges associated with image reconstruction at a single-frequency [7], occupy a very small footprint to facilitate dense spatial sampling of scattered fields, and radiate efficiently into the breast volume. Additionally, it is highly desired that the array be easily modeled in the forward simulations of our inverse scattering algorithm, which are conducted using the finite-difference time-domain method (FDTD) [3], [4].

Dual-band miniaturized patch antennas suitable for microwave breast imaging have been previously proposed [8]. These miniaturized patch antennas have a small footprint (28 mm x 29 mm) and operate within the frequency range of 0.5 GHz to 3.0 GHz. Frequencies below and above this range have limited spatial resolution and penetration depth, respectively. Our proposed array is composed of these dual-band miniaturized patch antennas.

978-1-4244-6051-9/11/$26.00 ©2011 IEEE

2. Array Design

We populate the four side panels of the array with 32 dual-band miniaturized patch antennas described in [8]. Figure 2 shows the geometry of the proposed 3-D sensor array. Individual antennas operate at two frequency bands centered at 1.37 GHz and 2.90 GHz. One of the goals of this investigation is to assess the extent to which the operating characteristics of the individual antenna elements are altered in the presence of other antenna elements as well as the breast.

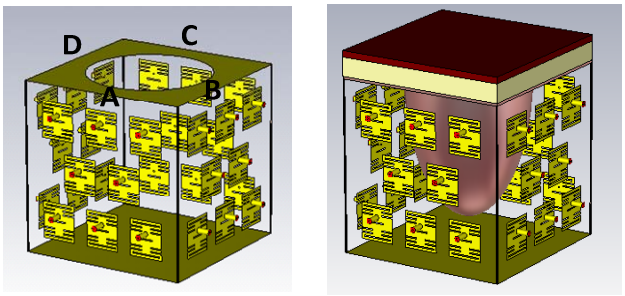

(a) (b)

Figure 2: Illustration of the proposed 3-D sensor array with (a) no phantom present (b) simple phantom present.

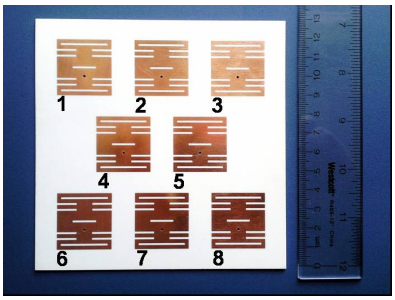

Figure 3: Photograph of a prototype of one 13 cm x 13 cm panel of the proposed array showing eight dual-band miniaturized (28 mm x 29 mm) antennas.

The top and bottom panels of the box contain metal planes that provide known boundary conditions at these locations of the imaging domain. The top metal plane includes an opening that allows the breast to be suspended in the imaging volume. Each panel is backed by a ground plane, which ensures unidirectional radiation into the imaging environment and provides isolation from external scatterers. The void between the array and the breast is filled with an immersion medium that provides an excellent impedance match with the tissue-stabilizing thermoplastic material, effectively making the thermoplastic invisible to the microwaves.

We focused on maximizing the number of antenna elements contained in each panel to increase the spatial sampling of scattered signals, while minimizing strong electromagnetic interaction between closely spaced elements. We first considered a panel arrangement that consisted of three rows of three antennas each. Simulations of transmission coefficients between pairs of antennas located in the same panel revealed that vertically adjacent elements exhibit a high level of mutual coupling. Consequently, we adopted a staggered-element arrangement, which reduced the mutual coupling between vertical antenna element pairs by about 6 dB. Figure 3 illustrates the proposed arrangement of eight elements on each panel forming a 32-element array. The antenna array panels are patterned on 32-mil-thick RO4003 substrates (Rogers Corp.). The patch antennas are probe-fed using the center conductor of an SMA connector.

An ellipsoidal breast phantom is introduced to the simulation domain as shown in Figure 2b. The pendant breast phantom is an 11.4 cm long ellipsoid with a 10 cm diameter circular base. The interior of the phantom is composed entirely of fatty tissue; the surface of the phantom includes a 2-mm-thick skin layer. For model completeness, the base of the breast also includes a 1.5-cm-thick subcutaneous fat layer and a 0.5-cm-thick muscle chest wall. The dispersive dielectric properties of breast fat, skin, and muscle are based on properties described in [9] and [10].

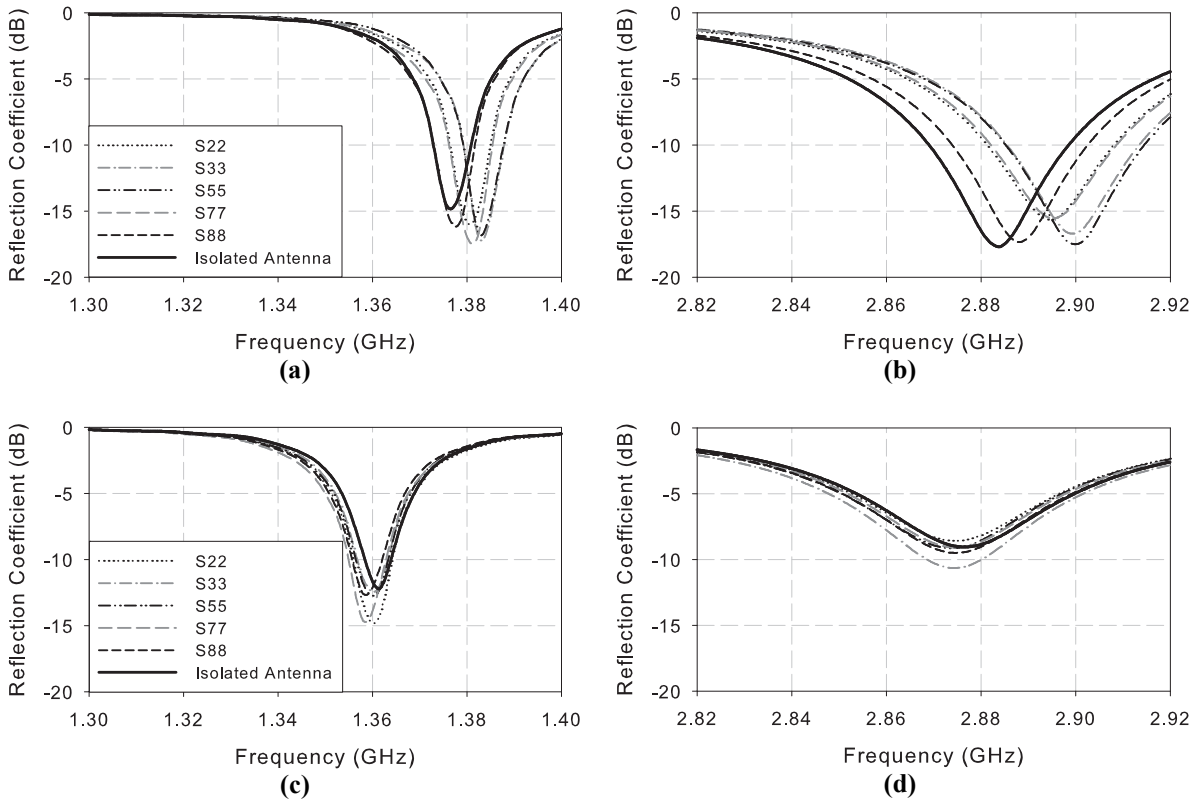

Figure 4: Simulated reflection coefficients (S_{ii}) for dual-band miniaturized patch antennas in a 3-D sensor array immersed in oil. 1st frequency band (left column) and 2nd frequency band (right column). [(a)-(b)] S_{ii} of antennas in sensor array with no phantom present and [(c)-(d)] S_{ii} of antennas in sensor array with simple phantom present. The bold black line corresponds to a single isolated antenna S_{ii}.

3. Results

We investigated the theoretical performance of the array using numerical simulations conducted with CST Microwave Studio. Here, we highlight the reflection coefficients of individual antenna elements. The magnitude of the simulated reflection coefficient of several miniaturized patch antennas are shown in Figure 4. We first obtained the simulated reflection coefficient for an isolated antenna, which is shown as the black solid line in Figure 4. The performance of each antenna element operating in the array environment was also simulated and the reflection coefficients for several antennas in a panel are shown in Figure 4. We compare these results with and without the ellipsoidal breast phantom described in Section 2.

In the case of a sensor array with no phantom present, the antenna elements exhibit dual-band operation with operating frequencies that deviate slightly from the isolated-antenna operating frequencies of 1.38 GHz (TM_{100}) and 2.88 GHz (TM_{300}). In the presence of the phantom, the center frequencies of operation shift down in frequency by about 1.5%. Additionally, when the phantom is present, the variation in center frequencies across the array is decreased.

4. Conclusions

The design of a compact 3-D sensor array composed of dual-band, miniaturized patch antennas for microwave breast imaging was presented. The array satisfies the space constraints of an existing clinical MRI setup to be used for co-registration of imaging results. Numerical simulations of the operating characteristics of the antenna elements contained in the array were performed. The radiating elements of the sensor array exhibit dual-band operation with no significant frequency deviation. The dual-band operation is maintained in the presence of an ellipsoidal breast phantom.

5. Acknowledgements

The authors would like to thank Prof. Wally Block, Prof. Sean Fain, and Matt Smith for sharing their expertise in designing an MRI patient support platform with removable breast coils. This work was supported by the National Science Foundation under a Graduate Fellowship, the National Institutes of Health under Grant No. R01 CA112398 awarded by the National Cancer Institute, and the Philip D. Reed Chaired Professorship.

6. References

1. P. M. Meaney, M. W. Fanning, T. Raynolds, C. J. Fox, Q. Q. Fang, C. A. Kogel, S. P. Poplack, and K. D. Paulsen, "Initial clinical experience with microwave breast imaging in women with normal mammography," *Academic Radiology*, vol. 14, no. 2, Feb. 2007, pp. 207–218.

2. C. Gilmore, A. Abubakar, W. Hu, T. M. Habashy, and P. M. van den Berg, "Microwave biomedical data inversion using the finite-difference contrast source inversion method," *IEEE Transactions on Antennas and Propagation*, vol. 57, no. 5, May 2009, pp. 1528–1538.

3. J. D. Shea, P. Kosmas, S. C. Hagness, and B. D. Van Veen, "Three-dimensional microwave imaging of realistic numerical breast phantoms via a multiple-frequency inverse scattering technique," *Medical Physics,* vol. 37, no. 8, Aug. 2010, pp. 4210-4226.

4. J. D. Shea, P. Kosmas, S. C. Hagness, and B. D. Van Veen, "Contrast enhanced microwave imaging of breast tumors: A computational study using 3-D realistic numerical phantoms," *Inverse Problems*, vol. 26, July 2010, 074009.

5. S. M. Aguilar, J. D. Shea, M. A. Al-Joumayly, B. D. Van Veen, N. Behdad, and S. C. Hagness, "Dielectric characterization of PCL-Based thermoplastic materials for microwave diagnostic and therapeutic applications," *IEEE Trans. Biomed. Eng.,* submitted.

6. Q. Fang, P. M. Meaney, and K. D. Paulsen, "Singular value analysis of the Jacobian matrix in microwave image reconstruction," *IEEE Trans. Antennas Propag.*, vol. 54, no. 8, Aug. 2006, pp. 2371–2380.

7. Q. Fang, P. M. Meaney, and K. D. Paulsen, "Microwave image reconstruction of tissue property dispersion characteristics utilizing multiple-frequency information," *IEEE Trans. Microw. Theory Tech.*, vol. 52, no. 8, Aug. 2004, pp. 1866–1875.

8. M. A. Al-Joumayly S. M. Aguilar, N. Behdad, and S. C. Hagness, "Dual-band miniaturized patch antennas for microwave breast imaging,"' *IEEE Antennas and Wireless Propagation Letters,* vol. 9, Mar. 2010, pp. 268-271.

9. M. Lazebnik, L. McCartney, D. Popovic, C. B.Watkins, M. J. Lindstrom, J. Harter, S. Sewall, A. Magliocco, J. H. Booske, M. Okoniewski, and S. C. Hagness, "A large-scale study of the ultrawideband microwave dielectric properties of normal breast tissue obtained from reduction surgeries," *Phys. Med. Biol.*, vol. 52, 2007, pp. 2637–2656.

10. S. Gabriel, R.W. Lau, and C. Gabriel, "The dielectric properties of biological tissues: III. Parametric models for the dielectric spectrum of tissues," *Phys. Med. Biol.*, vol. 41, 1996, pp. 2271–2293.